Environmental Science & Technology

Anthropogenic Impacts on the Atmosphere

Stable Sulfur Isotopes Revealed a Major Role of Transition-Metal-Ion Catalyzed SO Oxidation in Haze Episodes

Jianghanyang Li, Yanlin Zhang, Fang Cao, Wenqi Zhang, Meiyi Fan, Xuhui Lee, and Greg Michalski

Environ. Sci. Technol., **Just Accepted Manuscript** • DOI: 10.1021/acs.est.9b07150 • Publication Date (Web): 16 Jan 2020

Just Accepted

is published by the American Chemical Society. 1155 Sixteenth Street N.W., Washington, DC 20036

Stable Sulfur Isotopes Revealed a Major Role of Transition-Metal-Ion Catalyzed SO_2 Oxidation in Haze Episodes

Jianghanyang Li[1], Yan-Lin Zhang[2,*], Fang Cao[2], Wenqi Zhang[2], Meiyi Fan[2], Xuhui Lee[4,2] and Greg Michalski[1,3]

[1]Department of Earth, Atmospheric, and Planetary Sciences, Purdue University, West Lafayette, IN, USA

[2]Yale−NUIST Center on Atmospheric Environment, International Joint Laboratory on Climate and Environment Change (ILCEC), Nanjing University of Information Science and Technology, Nanjing 210044, China

[3]Department of Chemistry, Purdue University, West Lafayette, IN, USA

[4] School of Forestry and Environmental Studies, Yale University, CT, USA

Abstract

Secondary sulfate aerosols played an important role in aerosol formation and aging processes, especially during haze episodes in China. Secondary sulfate was formed via atmospheric oxidation of SO_2 by OH, O_3, H_2O_2 and transition metal catalyzed (TMI) O_2. However, the relative importance of these oxidants in haze episodes was strongly debated. Here we use stable sulfur isotopes ($\delta^{34}S$) of sulfate aerosols and a Rayleigh distillation model to quantify the contributions of each oxidant during a haze episode in Nanjing, a megacity in China. The observed $\delta^{34}S$ values of sulfate aerosols showed a negative correlation with sulfur oxidation ratios, which was attributed to the sulfur isotopic fractionations during the sulfate formation processes. Using the average fractionation factor calculated from our observations and 0-D atmospheric chemistry modeling estimations, we suggest that OH oxidation was trivial during the haze episode, while the TMI pathway contributed 49±10% of the total sulfate production and O_3/H_2O_2 oxidations accounted for the rest. Our results displayed good agreement with several

atmospheric chemistry models that carry aqueous and heterogeneous TMI oxidation pathways, suggesting the role of the TMI pathway was significant during haze episodes.

Abstract Art

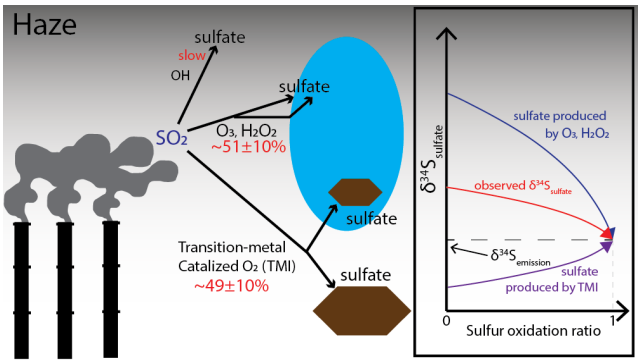

Introduction

Haze episodes in Chinese cities are adversely affecting the environment and the health of millions of residents. Most haze episodes are characterized by high concentrations and fast accumulation of aerosol sulfate[1–4], which could contribute to as much as 45% of total aerosol mass. Over 90% sulfate in haze episodes is secondary sulfate, i.e., sulfate produced from SO_2 oxidation in the atmosphere via 1) gas phase oxidation by OH radical[5]; 2) aqueous oxidation by H_2O_2, O_3, and Transition Metal Ions (TMI) catalyzed O_2[6–12]; and 3) heterogeneous oxidation on the surface of aerosols, cloud droplets and mineral dusts by the same oxidants as aqueous oxidation[1,13–16]. Some studies[11,12,14,17,18] also suggested the NO_2 might played an important role during the formation of aerosol sulfate, probably by facilitating TMI oxidation[19], which is based on an experimental study[20] that demonstrated the direct oxidation of SO_2 by NO_2 was several orders of magnitude slower than gas phase OH oxidation. However, aerosol collected from several Chinese urban areas (e.g., Nanjing) were acidic[21], suggesting NO_2 oxidation might not be important in these regions. Furthermore, a recent GEOS-Chem modeling study[22] has suggested NO_2 oxidation contributed less than 2% of total sulfate production during haze episodes. While the gas phase oxidation rate of SO_2+OH is well-constrained, there are many uncertainties in quantifying the rates of aqueous and heterogeneous SO_2 oxidation. One of the ongoing debates is the relative contribution of each SO_2 oxidation pathway during haze episodes. Some[8,12,13] have suggested that O_3 and H_2O_2 oxidation of SO_2 in aqueous phase contributed to the majority of total sulfate production, while the TMI pathway played a minor role. Others[17,23] have countered that the TMI pathway is likely also very important in highly polluted regions. Therefore, addressing this debate is essential to unravel the complex atmospheric sulfur chemistry in haze episodes.

Atmospheric chemistry models are often used to study the sulfate chemistry but many models have uncertainties in parameterizing aqueous and heterogeneous SO_2 oxidation chemistry under haze conditions, resulting in underestimation of sulfate formation rates during haze episodes[1,24–26]. One of the biggest uncertainties is the pH of aerosol water: several studies had attempted to calculate the aerosol water pH in Beijing[12,17,27–29] using the same model (ISORROPIA II). Depending on assumptions about whether the aqueous phase is at thermodynamic stable state[17,30], the calculated pH was either 3-5 or >5.5. This uncertainty greatly impacts the quantification of aqueous SO_2 oxidation rate[31]. A pH increase of 1 unit will increase the O_3 oxidation rate by two orders of magnitude but decrease the TMI oxidation rate by 2-3 orders of magnitude. Conversely, the rate of SO_2 oxidation by H_2O_2 is insensitive to changing pH. Additionally, atmospheric models usually quantify the rate of TMI oxidation pathway using modeled aerosol Fe and Mn concentrations[10]. However, studies[9,32] have suggested that aerosol surface type, temperature, irradiation, and the existence of other transition metals in aerosol water, could alter the rate of TMI oxidation by as much as two orders of magnitude, adding more complexity to this question. Therefore, in order to 1) reduce the uncertainties in atmospheric models and 2) verify the performance in models during haze episodes, an alternative approach is needed to assess the relative importance of each oxidation pathway.

The isotopic composition of sulfate aerosols has been used to determine the formation processes of sulfate aerosols. The mass-independent fractionation signals (non-zero $\Delta^{17}O$, where $\Delta^{17}O = \delta^{18}O-0.52*\delta^{17}O$) of oxygen isotopes in sulfate are often used to estimate the contributions of $SO_2 + O_3$ and H_2O_2 to the formation of sulfate aerosols[10,17,33], since $SO_2 + O_3$ and $SO_2 + H_2O_2$ are the only known two pathways that produce non-zero $\Delta^{17}O$ values in sulfate[34]. Sulfate formed via $SO_2 + O_3$ yields $\Delta^{17}O$=6.5‰ and sulfate formed via $SO_2 + H_2O_2$ shows $\Delta^{17}O$ = 0.7‰. This

method can easily identify the significant contribution of SO_2+O_3 pathway when high $\Delta^{17}O$ (>3‰) are measured in sulfate samples. There is significant uncertainty, however, when interpreting sulfate aerosols with low $\Delta^{17}O$ values (<1‰). Unfortunately, most sulfate aerosols in haze episodes show $\Delta^{17}O$ < 1‰[17,22], suggesting limited contribution from SO_2+O_3 pathway, but the relative importance of the SO_2 + H_2O_2 pathway and the TMI pathway is still unclear. Therefore, solely using $\Delta^{17}O$ probably cannot precisely distinguish the contributions from the SO_2 + H_2O_2 and the TMI pathways in haze episodes.

Stable sulfur isotopes ($\delta^{34}S$) have the potential to indicate the formation pathways of sulfate aerosols. The fractionation factors for sulfur isotopes during multiple oxidation pathways (SO_2+OH, SO_2+H_2O_2/O_3, TMI) have been determined experimentally[35–37]. Yet to date there are few studies using sulfate $\delta^{34}S$ values to interpret the oxidation pathways of SO_2[35,38,39]. This is because the $\delta^{34}S$ values of sulfate aerosols ($\delta^{34}S_{sulfate}$) are simultaneously controlled by the $\delta^{34}S$ value of SO_2 sources[40,41] ($\delta^{34}S_{emisssion}$) and the kinetic and equilibrium isotope effects occurring during the oxidation process. The $\delta^{34}S_{emisssion}$ strongly depends on the origin of SO_2 therefore can be difficult to constrain. However, during haze episodes, SO_2 generally originates from local sources because air stagnation limits long range transport, and the $\delta^{34}S_{emission}$ can be well-constrained using local SO_2 emission inventory and observations. Thus, the differences between $\delta^{34}S_{emission}$ and $\delta^{34}S_{sulfate}$ can be attributed to the isotopic fractionations during the oxidation processes, which are controlled by the oxidation pathways. This isotopic fractionation during SO_2 oxidation should be treated as a Rayleigh distillation process[42] since isotopic exchange between the product sulfate and the reactant SO_2 is minimal[35]. Currently, many studies have measured the $\delta^{34}S_{sulfate}$ in Chinese megacities[38,39,43–47] in order to understand the sources of atmospheric SO_2 and the secondary sulfate aerosols. Some works also have measured $\delta^{33}S$ and

100 $\delta^{36}S^{47-51}$ to further constrain the origins of atmospheric SO_2. However, the differences between
101 $\delta^{34}S_{emission}$ and $\delta^{34}S_{sulfate}$, as well as the isotopic fractionation process during the formation of
102 sulfate, were rarely discussed and poorly understood. Here, we used the Rayleigh distillation
103 model to investigate the sulfur isotopic fractionations of sulfate aerosols collected during a haze
104 episode in winter 2015 at Nanjing, China, to understand the relative contribution of each SO_2
105 oxidation pathway.
106
107 **Materials and Methods**
108 Sulfate aerosols were sampled during a severe haze episode in winter 2015, in Nanjing,
109 Peoples Republic of China. The sampling site was located at the Agrometeorological station in
110 Nanjing University of Information Science and Technology (NUIST). Two large industrial areas
111 are located ~10 km northeast and ~5 km southwest of the sampling site, and downtown Nanjing
112 is 20 km to the southeast (Fig. 1). A high-volume aerosol sampler equipped with a pre-
113 combusted quartz filter was used to collect ambient aerosol samples (<2.5 μm in diameter, $PM_{2.5}$)
114 from January 22th to 28th at a flow rate of 1 m^3/min, and the filter was replaced every 3 hours.
115 Once the aerosol samples were collected, the filters were wrapped in aluminum foil, sealed in
116 air-tight polyethylene bags and stored in freezer to minimize sample loss or evaporation. To
117 determine the anion, cation concentrations of filter samples, a quarter of each filter was cut and
118 the soluble components on the filter were dissolved into 50 mL of Millipore water (18.2 MΩ).
119 Then the solution was sonicated for at least 30 min to ensure all the soluble ions were completely
120 dissolved. Subsequently the solutions were filtered through 0.45 μm filters to remove insoluble
121 material. An aliquot of each solution was taken and used to measure the anion and cation
122 concentrations using a Dionex ICS 5000+ at NUIST following standard ion chromatography (IC)

procedure[52] while the rest solutions were kept frozen. The analytical uncertainty for the IC analysis was ±5%. Meteorological data (wind speed and direction, temperature, RH) were obtained from an automatic meteorological station next to the sampling site. Concentrations of pollutants ($PM_{2.5}$, NO, NO_2, O_3, CO and SO_2) were obtained from the Environmental Supervising Station at Pukou district, Nanjing, ~15 km away from the sampling site.

Sulfur isotopic analysis was conducted at the Purdue Stable Isotope Laboratory at Purdue University. The sulfur isotopic analysis follows the procedure in Li et al. (2018)[40]. Another quarter of each sample was again dissolved into 10 mL of Millipore water (18.2 MΩ), and each solution was sonicated for 30 min to completely dissolve all the sulfate on the filter. To completely precipitate $BaSO_4$, 1 mL of 5% $BaCl_2$ solution and subsequently 0.5 mL of 37% HCl were added into each sample solution. Between 0.1 to 0.5 mg of $BaSO_4$ precipitate was then weighed into tin boats and combusted at 980 °C in an elemental analyzer (Costec), then the product SO_2 was directed into an Isotope Ratio Mass Spectrometer (ThermoDeltaV) to measure the $\delta^{34}S$ values. The analytical uncertainty of the sulfur isotopic analysis was ±0.1‰ inferred from IAEA-SO5 and IAEA-SO6 external standards.

Results and discussions

The haze episode occurred in Nanjing during winter 2015 and was characterized by high $PM_{2.5}$, high sulfate concentrations, and air stagnation. Prior to the haze episode (between Jan. 18 and Jan. 21, 2015) the $PM_{2.5}$ concentrations averaged 83.1 μg/m^3. The haze episode began between Jan. 22 00:00 and Jan. 23 12:00 when $PM_{2.5}$ became elevated, with concentrations of 109.3±16.0 μg/m^3. $PM_{2.5}$ continued increased to an average of 159.4 μg/m^3 between the 22nd and 26th of Jan. during which two significant $PM_{2.5}$ accumulation events were observed. The first

accumulation (Event I, Fig. 2A) started on Jan. 23 13:30 and lasted for 33 hours, during which the $PM_{2.5}$ concentration more than doubled, from 104.0 μg/m^3 to 268.3 μg/m^3. This was followed by a 2-hour light precipitation (~1 mm), which rinsed out some of the $PM_{2.5}$, decreasing its concentration to 134.0 μg/m^3 within 15 hours. A subsequent $PM_{2.5}$ accumulation period (Event II) occurred within 24 hours, when the $PM_{2.5}$ concentration increased from 134.0 to 243.7 μg/m^3. Sulfate aerosol concentrations followed trends similar to $PM_{2.5}$ concentrations and mirrored the two rapid accumulation events. During Event I, sulfate have increased from 21.0 μg/m^3 to 58.5 μg/m^3 in 27 hours (accumulation rate of 1.39 μg/m^3/h) and during Event II sulfate increased from 24.4 μg/m^3 to 71.8 μg/m^3 within 21 hours (accumulation rate of 2.26 μg/m^3/h). Primary sulfate (includes soil sulfate, sea-salt sulfate, and sulfate directly emitted with SO_2) was determined to be trivial during these events. Low concentrations of Ca^{2+} (1.88±1.09 μg/m^3) and Na^+ (0.97±0.86 μg/m^3) in the aerosols indicated contribution of sulfate from soil entrainment[53] (SO_4^{2-}/Ca^{2+}=0.18) and sea-salt aerosols[54] (SO_4^{2-}/Na^+=0.25) should be less than 0.58 μg/m^3, corresponding to <2% of total sulfate observed. Primary sulfate emitted with SO_2 during coal burning has been estimated to be only <4% of SO_2 emission[10,55], which based on observed SO_2 concentrations, would average at 1.66 ± 0.6 μg/m^3 during the sampling period (Fig. 2A). Thus, total primary sulfate only contributed for <6% of total sulfate, indicating most was secondary sulfate (i.e. SO_2 oxidation). Additionally, the wind speed during the entire haze episode averaged at 1.03±0.71 m/s with a maximum 3-h wind speed of 2.58 m/s (wind rose in Fig. 1), indicating air stagnation. Considering the short lifetime[31] of atmospheric SO_2 (~12 h) and aerosols (~5 days) and the relatively low sulfur emissions outside of Nanjing within 200 km inferred from SO_2 emission inventory[56], long-range transportation of $SO_{2(g)}$ and sulfate should be minor, thus local SO_2 emissions and oxidation within Nanjing should be the dominant source of aerosol sulfate.

The measured $\delta^{34}S_{sulfate}$ values were significantly higher than the estimated $\delta^{34}S_{emission}$ value in Nanjing[38,39,44], showing a ~5‰ variation throughout the sampling period, and displayed a negative correlation with SO_2 Oxidation Ratio (SOR = $SO_4^{2-}/(SO_4^{2-}+SO_2)$). $\delta^{34}S_{sulfate}$ values (Fig. 3A) in our samples ranged from +4.3‰ to +9.4‰ with an average of 6.2‰, similar to the values observed in a number of other Chinese megacities[23,44–46]. Because of the air stagnation, the SO_2 likely originated from local emissions, the majority of which in Nanjing was coal combustion with a $\delta^{34}S$ value of 3.0±0.9‰[43]. Several studies have measured the $\delta^{34}S$ values of both SO_2 and sulfate simultaneously at Nanjing, showing that the $\delta^{34}S_{emission}$ ($\delta^{34}S_{emission}=\delta^{34}S_{SO2}*(1-SOR)+\delta^{34}S_{SO42-}*SOR$) was +4.0±0.1‰[44] in 1997 and 2.4±0.6‰[38] in fall 2014. Chen et al. (2017)[39] have analyzed the $\delta^{34}S_{emission}$ in Nanjing prior to our sampling period (daily SO_2 and sulfate samples from Jan. 1 to Jan. 23 while this work sampled 3-hour sulfate samples from Jan. 22 to Jan. 26) and found a constant $\delta^{34}S_{emission}$ value of 2.7±1.0‰[39]. Therefore, we suggest that the $\delta^{34}S_{emission}$ value during our sampling period should also be 2.7±1.0‰ (Fig. 3A). These values are in good agreement with the SO_2 emission inventory[56] which suggested that over 96% SO_2 emission in winter in the Nanjing area was from industrial and coal burning power plants, which had $\delta^{34}S$ values of 3±3‰[44,57]. The measured $\delta^{34}S_{sulfate}$ values were significantly higher than the $\delta^{34}S_{emission}$, suggesting enrichment of ^{34}S in the sulfate and hence a depletion of ^{34}S in the remaining SO_2. This phenomenon has been observed in other studies, where the $\delta^{34}S$ values of aerosol sulfate were usually 0-8‰ higher than the coexisting SO_2[38,39,41,44,58,59] but this phenomena was not quantitatively explained. Also, the $\delta^{34}S_{sulfate}$ values showed a ~5.1‰ variation throughout the sampling period. If the $\delta^{34}S_{emission}$ remain constant during our sampling period, this variation could be explained as a result of sulfur isotopic fractionation during the oxidation process. Furthermore, we observed a negative correlation (slope=-6.2, r=0.6, Fig 3A, B)

between SOR and $\delta^{34}S$ value of sulfate in our samples, indicating that as oxidation of SO_2 progressed the $\delta^{34}S$ values of sulfate decreased, making them approach $\delta^{34}S_{emission}$ (by isotope mass balance). This negative correlation supported our hypothesis that the elevated and variable $\delta^{34}S_{sulfate}$ values should be attribute to the isotopic fractionation during SO_2 oxidation processes.

The discrepancies between $\delta^{34}S_{sulfate}$ and $\delta^{34}S_{emission}$ (therefore, $\delta^{34}S_{SO2}$) values have been observed, especially at low SOR levels. Forrest and Newman (1973)[59] measured $\delta^{34}S$ values of $SO_{2(g)}$ and sulfate particles in polluted environment with very low SOR (average SOR=9.9% among 3 experiments), the $\delta^{34}S_{sulfate}$ values were ~1.5-2.5‰ higher than the $\delta^{34}S_{SO2}$ values. Saltzman (1983)[41] conducted similar experiment at Hubbard Brook Experimental Forest, New Hampshire, USA, observed ~3‰ difference between $\delta^{34}S_{sulfate}$ and $\delta^{34}S_{SO2}$ values when the SOR were <40%. Later studies by Guo et al. (2016)[38] and Chen et al. (2017)[39] have suggested the $\delta^{34}S_{sulfate}$-$\delta^{34}S_{SO2}$ values at Nanjing ranged between ~1-7‰ during fall 2014 and winter 2015. These differences have suggested that $\delta^{34}S_{sulfate}$ may deviate from the $\delta^{34}S_{emission}$ by several permil, especially when the SOR value was low. This deviation might complicate the use of $\delta^{34}S_{sulfate}$ to calculate the sources of SO_2 in urban regions, since most urban (anthropogenic) SO_2 sources have a narrow range of $\delta^{34}S$ values[45,57] (+1-+11‰), which could be potentially altered by the isotopic fractionations during the formation of sulfate when SOR was low. This uncertainty might be reduced by analyzing other minor sulfur isotopes (^{33}S, ^{35}S, ^{36}S)[47–51], but this is beyond the scope of our work. Therefore, extra cautious must be taken when using $\delta^{34}S$ values to estimate the sources of SO_2 in urban environment with low SOR.

The observed differences in $\delta^{34}S_{sulfate}$ and $\delta^{34}S_{emission}$ values can be explained using a Rayleigh distillation model, and to the isotopic enrichment factor ($\varepsilon = (\alpha-1)*1000‰$) for the total oxidation processes can also be quantified. The Rayleigh distillation model[42,60] is used to

calculate the kinetic isotopic fractionation of a reaction (A→B) in an open system by assuming no isotopic exchange between A and B. In aqueous solution, $SO_{2(g)}$ dissolving into aerosol water was 2-3 order of magnitude faster than the subsequent oxidation into SO_4^{2-}, thus the isotopic fractionation should be controlled by the kinetic isotopic effect occurring during any aqueous SO_2 oxidation process[35]. In this model, the $\delta^{34}S$ value of SO_2 is a function of $\delta^{34}S_{emission}$, fraction (f) of remaining SO_2 (f = 1-SOR), and observed fractionation factor of the oxidation process (ε_{obs}):

$$\delta^{34}S_{SO2} = \delta^{34}S_{emission} + \ln(f) * \varepsilon_{obs} \quad (1)$$

Thus $\delta^{34}S_{sulfate}$ is:

$$\delta^{34}S_{sulfate} = \delta^{34}S_{emission} - \varepsilon_{obs} * \ln(f) * f/(1-f) \quad (2)$$

Using the observed $\delta^{34}S_{sulfate}$, f, and the estimated $\delta^{34}S_{emission}$ during our sampling period (2.7‰±1.0‰), we found the ε_{obs} values ranged from 2.2‰ to 10.0‰ (Fig. 3B) with an average value of +5.3‰±1.8‰ (1σ).

This changing ε_{obs} value suggest that multiple SO_2 oxidation pathways have contributed to the observed sulfate accumulation. At 273K (average temperature during the sampling period), OH oxidation enriches ^{34}S in the product sulfate with an enrichment factor (ε_{OH}) of +11.0‰[35], and oxidation by TMI pathway depletes ^{34}S (ε_{TMI}=-5.0‰) in the product sulfate with a ε_{TMI} value of -5.0‰[35,36]. Several laboratory experiments[35–37] measured the ε values of $SO_2 + O_3$ and $SO_2 + H_2O_2$, and these two pathways showed similar ε values ranging from +15.1‰ to +17.4‰. Therefore, here we use $\varepsilon_{O3/H2O2}$ = +15.1‰ to represent the combined isotopic effect of O_3 and/or H_2O_2 pathways. Since the variation of temperature during the entire sampling period was small (standard deviation of ±3.7 K), the variations of the fractionation factors (<1‰) was insignificant

237 comparing to the differences between the fractionation factors (~20‰). Therefore, in the
238 following calculation we assume the fractionation factors are constants. The ε_{obs} value does not
239 agree with any of the laboratory-determined ε values, suggesting none of the pathway had a
240 dominant role in the formation of the sulfate. Instead, the ε_{obs} should be a result of mixing of
241 multiple oxidation pathways:

242 $$\varepsilon_{obs} = \varepsilon_{O3/H2O2} * f_{O3/H2O2} + \varepsilon_{TMI} * f_{TMI} + \varepsilon_{OH} * f_{OH} \quad (3)$$

243 In which ε_i and f_i are the enrichment factor and the contribution of pathway *i*, and $f_{O3/H2O2} + f_{TMI} +$
244 $f_{OH} = 1$.

245 The sulfate formed via the gas phase SO_2+OH pathway was calculated to be unimportant.
246 Concentrations of OH radical were first obtained using a 0-D atmospheric chemistry model
247 coupled with time-dependent photochemistry. The model used Tropospheric Ultraviolet and
248 Visible (TUV) radiation model[61] to determine the molecular photolysis frequencies (j values) for
249 the major molecules (O_3, NO_2, NO_3, HONO, N_2O_5, H_2O_2, and other organic molecules) during
250 the sampling period a time step of 3 hours. Subsequently calculated j values were incorporated
251 into a 0-D atmospheric chemistry model driven by "Regional Atmospheric Chemistry Modeling"
252 (RACM) mechanism[62]. The model then calculated time-dependent OH radical concentrations
253 (Fig. S1) using average concentrations of trace gases (O_3, H_2O, NO_2, SO_2, CO, CH_4) during the
254 pollution period. The OH concentrations display clear diurnal variation, with the peak
255 concentration of $1.35*10^6$ molecules/cm^3 at noon, and a daily average value of $0.31*10^6$
256 molecules/cm^3, similar to the observed winter OH concentrations in other urban areas[63,64]. The
257 reaction rates of gas phase SO_2 oxidation (SO_2+OH) were then calculated using:

258 $$d[SO_4^{2-}]/dt = k * [SO_2] * [OH] \quad (4)$$

in which k is the reaction constant[5] at 273K ($1.5*10^{-12}$ $molecule^{-1}*cm^3*s^{-1}$), [$SO_2$] and [OH] are observed SO_2 concentrations and calculated OH concentrations. The results (grey line in Fig. 2B) suggest that the OH oxidation rate averaged at 0.05 $\mu g/m^3/h$ during the entire sampling period and the maximum oxidation rate with highest OH concentration at noon was only 0.3 $\mu g/m^3/h$. Since the measured sulfate accumulation rates were 1.3 and 2.1 $\mu g/m^3/hr$ during the two accumulation events, respectively, and assuming a negligible sulfate dry deposition of 0.1 cm/s[65] and an average boundary layer height of 600 m, then the sulfate production rates during the two events were 1.55 and 2.38 $\mu g/m^3/hr$. These estimated sulfate production rates are 26-46 times faster than the average OH oxidation rate. Similar low sulfate production via gas phase oxidation was also inferred during winter haze episodes in Beijing[17]. This low contribution (2-3%) of gas phase sulfate production was probably because of a combination of weak photochemistry in winter, high aerosol concentration that scattered light, and extremely high heterogeneous and aqueous oxidation in haze episodes[11,66,67]. Therefore, O_3, H_2O_2 and TMI pathways should be the dominate contributors to the observed high sulfate production, and Eq. 3 can be simplified as:

$$\varepsilon_{obs} = \varepsilon_{O3/H2O2} * f_{O3/H2O2} + \varepsilon_{TMI} * f_{TMI} \quad (5)$$

Eq. 5 can be used to estimate the role of heterogeneous and aqueous oxidations of $SO_{2(g)}$ by O_3, H_2O_2 and TMI-catalyzed O_2 that were likely to be responsible for the fast accumulation of sulfate aerosols during the haze episode. This hypothesis is further confirmed by applying a pseudo-first-order uptake process to estimate heterogeneous and aqueous sulfate production[1]. This approach treats SO_2 oxidation on/in the aerosols as a first order uptake reaction on the surface of the aerosols:

$$SO_{2(g)} + \text{aerosol} \rightarrow \text{sulfate}$$

Its rate is expressed as[1,17,68]:

$$d[SO_4^{2-}]/dt_{het}=(R_a/D_g+4/\gamma\nu)^{-1}*S_a*[SO_2] \quad (6)$$

in which D_g ($2*10^{-5}$) is SO_2 diffusion coefficient[68], ν (300 m^2*s^{-1}) is SO_2 mean molecular velocity[68], R_a is the effective radius of aerosols, which is estimated using the following equation that was empirically derived from two haze episodes in Beijing[2]:

$$R_a =(0.254*[PM_{2.5}]/(\mu g/m^3)+10.259)*10^{-9}\ m \quad (7)$$

S_a is the aerosol surface area density (cm^2/cm^3) estimated using the average aerosol effective radius and average density (ρ) of $PM_{2.5}$ (1.5 g/cm^3):

$$S_a = [PM_{2.5}] * 3 / (R_a*\rho) \quad (8)$$

and γ is the SO_2 uptake coefficient. Although laboratory determined γ values of SO_2 uptake can vary by several orders of magnitude depending on the surface property, particle compositions, temperature and RH, previous modelling work have shown that setting the average γ values as a function of relative humidity[1] would best match modeled sulfate to observations:

$$\gamma = \max(2.0*10^{-5}, 6.0*10^{-7}*RH(\%)-1*10^{-5}) \quad (9)$$

The calculated sulfate production rates ranged from 0.8-5.2 $\mu g/m^3/h$ with a mean value of 2.3 $\mu g/m^3/h$ during the sampling period (Fig. 2B), similar to the observed sulfate accumulation rates (1.5 and 2.1 $\mu g/m^3/h$). Therefore, this calculation implies that heterogeneous and aqueous oxidation via O_3, H_2O_2 and TMI pathways were the main sources of sulfate during the haze episode. The overall calculated sulfate production rate agree well with the observed data, but this approach seems to be overestimating the sulfate production during Event I by ~80% (2.79 $\mu g/m^3/h$ vs. observed 1.55 $\mu g/m^3/h$) and underestimating the sulfate production in Event II by ~44% (1.32 $\mu g/m^3/h$ vs. observed 2.38 $\mu g/m^3/h$). Since the $PM_{2.5}$ mass and hence aerosol surface area were similar between the two events (141±41 $\mu g/m^3$ in Event I vs. 171±24 $\mu g/m^3$ in Event II) but the RH in Event II (81±2%) was higher than Event I (57±17%), and that the SO_2 uptake

coefficient is a function of RH, we suggest this discrepancy might be due to the over/under estimation of SO_2 uptake coefficient at low/high RH. The calculated SO_2 uptake coefficient ranged from $2*10^{-5}$ to $5*10^{-5}$, but experimental data has shown that these coefficients are a function of aerosol surface material. SO_2 uptake coefficients can be as low[69] as $0.41*10^{-5}$ on Sahara dust or as high[70] as $6.6*10^{-5}$ on iron oxides. Therefore, we suggest the pseudo-first-order uptake process estimation[1] showed general agreement with observed average production rate, although it is possible to under/overestimate the uptake coefficients (therefore oxidation rate) over a short time period at certain conditions because of the heterogeneity of aerosol compositions.

These calculations suggest that sulfate in the haze episode was primarily controlled by the heterogeneous and aqueous oxidation via O_3, H_2O_2, and TMI pathways, enabling us to use the ε_{obs} and Eq. 5 to estimate the contributions of the oxidation pathways. The overall ε_{obs} value (+5.3 ± 1.8‰) falls in between $\varepsilon_{O3/H2O2}$ and ε_{TMI} values, indicating both O_3/H_2O_2 and TMI pathways played important roles in the oxidation process. Using Eq. 5 we determined the overall contributions from TMI and O_3/H_2O_2 pathways (Fig. 3C) were roughly equal (f_{TMI} = 49±10%, $f_{O3/H2O2}$= 51±10%) during the haze episode. Notably, however, there were two time periods (at the end of $PM_{2.5}$ accumulation events I and II) when decreases in the ε_{obs} values were observed. In the first time period (Jan. 24, 6:00 to 18:00), sulfate concentration increased by ~100%, SOR remained steady, while the $\delta^{34}S_{sulfate}$ values decreased from 8.4‰ to +4.6‰. The calculated ε_{obs} values, thus, have decreased from 7.2‰ to 2.8‰, suggesting the TMI pathway have played a more important role during this process. The second time period (Jan. 25, 12:00 to Jan. 26, 3:00) was similar, when sulfate concentration increased by ~180% and the ε_{obs} value decreased from 9.9‰ to 3.4‰. Both events were associated with high $PM_{2.5}$ and low O_3 concentrations. The

decreased ε_{obs} values suggested elevated contributions of TMI pathway (accounting for 57-62% of sulfate production). The increased TMI pathway contribution likely resulted from a combination of two factors. First, the high aerosol concentrations, which likely provided high aerosol surface area and high amount of transition metal ions (e.g., Fe, Mn, Cu, Zn, Pb) from local industrial emission[71], which could enhance the rate of TMI oxidation. The second, O_3/H_2O_2 oxidation rate was likely decreased due to decreased O_3 concentrations and liquid water content. The average O_3 concentrations (6.2 and 5.0 μg/m^3) and RH (51% and 65%) during these two periods were significantly lower than the rest of the haze episode (averaging 13.0 μg/m^3 O_3 and 81% RH), which might reduce the oxidation rate of O_3/H_2O_2. However, since it is difficult to quantitatively determine the rate of TMI pathway and the accurate pH of aerosol water therefore the rate of O_3 oxidation, either factor or both factors could be the dominant cause. Future experimental work is needed to separately investigate the effects of aerosol surface area, transition metal ion concentrations, RH, O_3 concentration etc., to each oxidation pathway.

The significant contribution from the TMI pathway (49±10%) suggest an elevated role of the TMI pathway during the rapid formation of sulfate aerosols in the haze episode, showing general agreement with atmospheric chemistry modeling studies. Globally the TMI pathway was estimated to contributed to 9-18% of total aerosol production[8,10], in most regions in China (including Nanjing), model simulations suggested that TMI had played a more important role, contributing to ~20-50% of total sulfate production[10]. Harris et al. (2013)[35] also pointed out that at least 35% of sulfate in several Chinese cities[44] was produced via the TMI pathway. During haze episodes, the contributions of the TMI pathway among the heterogeneous and aqueous oxidations seems to increase: a recently-developed modeling study[22] suggest the TMI pathway was responsible for as much as 80% of total heterogeneous and aqueous sulfate production

during haze episodes in Beijing, and oxygen isotopic evidence suggested similar contributions (66-73%)[17]. Furthermore, field observation work at another heavily polluted region (Fort McMurray, Alberta, Canada) also implied the importance of the TMI pathway during the formation of secondary sulfate[72]. Our study had pointed out that, the TMI pathway was an important but probably not sole sulfate formation pathway during the haze episodes, and its contribution was likely elevated during the haze episodes. The increased contribution of the TMI pathway during haze episodes might originate from a combination of high aerosol surface, high atmospheric liquid water content and dust flux. In the meantime, the O_3 and/or H_2O_2 also played a major role in the formation of sulfate aerosols despite their lower-than-typical concentrations. Therefore, in order to improve the simulation of sulfate aerosol formation, all the above reactions (aqueous O_3, H_2O_2, TMI oxidations and heterogeneous O_3, H_2O_2, TMI oxidations) should be carefully parameterized in atmospheric chemistry models.

Corresponding author

Yan-Lin Zhang, dryanlinzhang@outlook.com

Notes

The authors declare no competing interest.

Acknowledgement

We thank funding support from National Nature Science Foundation of China (No. 91644103), National Key R&D Program of China (No. 2017YFC0212704 and 2017YFC0210101), the Provincial Natural Science Foundation of Jiangsu (No. BK20180040) and Jiangsu Innovation & Entrepreneurship Team, the National Science Foundation of U.S.,

373 Purdue Climate Change Research Center and the Advanced Study Program from National Center
374 for Atmospheric Research, U.S.

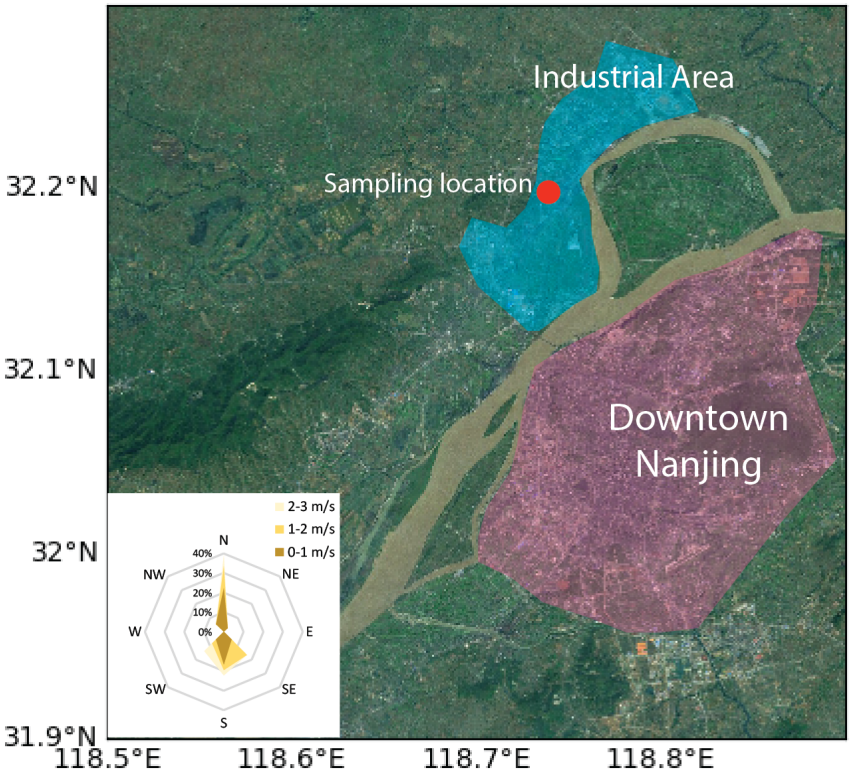

375

376 Fig 1. The sampling location was in between two large industrial areas (blue) and downtown
377 Nanjing (red) is 20 km to the southeast. Wind rose during the sampling period is shown at the
378 lower left corner: the highest 3-hr wind speed was < 3m/s, indicating air stagnation.

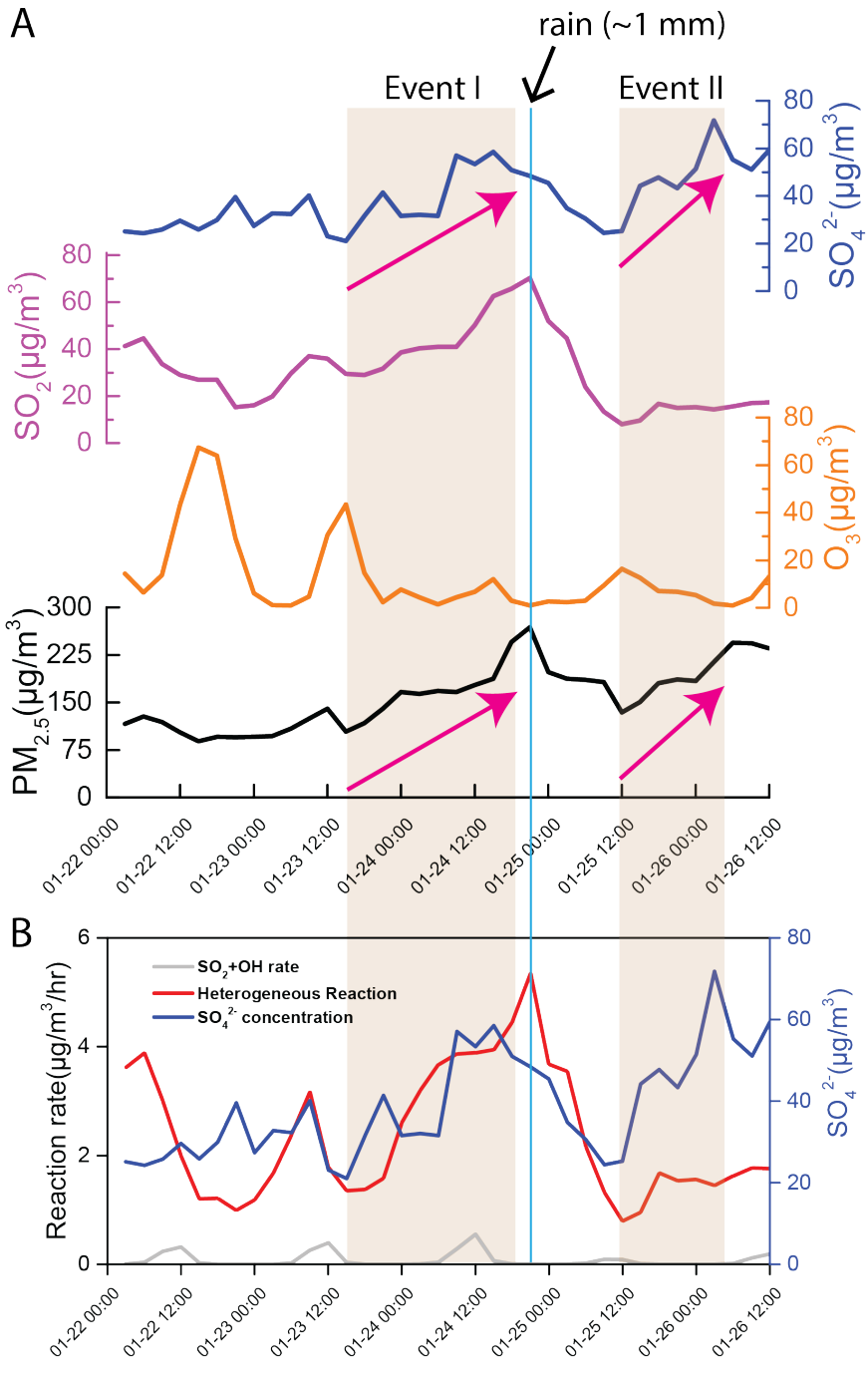

379

380 Fig. 2 A) Concentrations of sulfate, SO_2, O_3 and $PM_{2.5}$ during the haze episode. Shaded areas
381 indicated two rapid $PM_{2.5}$ and sulfate accumulation events, blue line indicated a small rain event
382 during the sampling period; B) calculated reaction rates of SO_2+OH (grey) and heterogeneous
383 reaction (red) plotted with sulfate concentrations (blue).

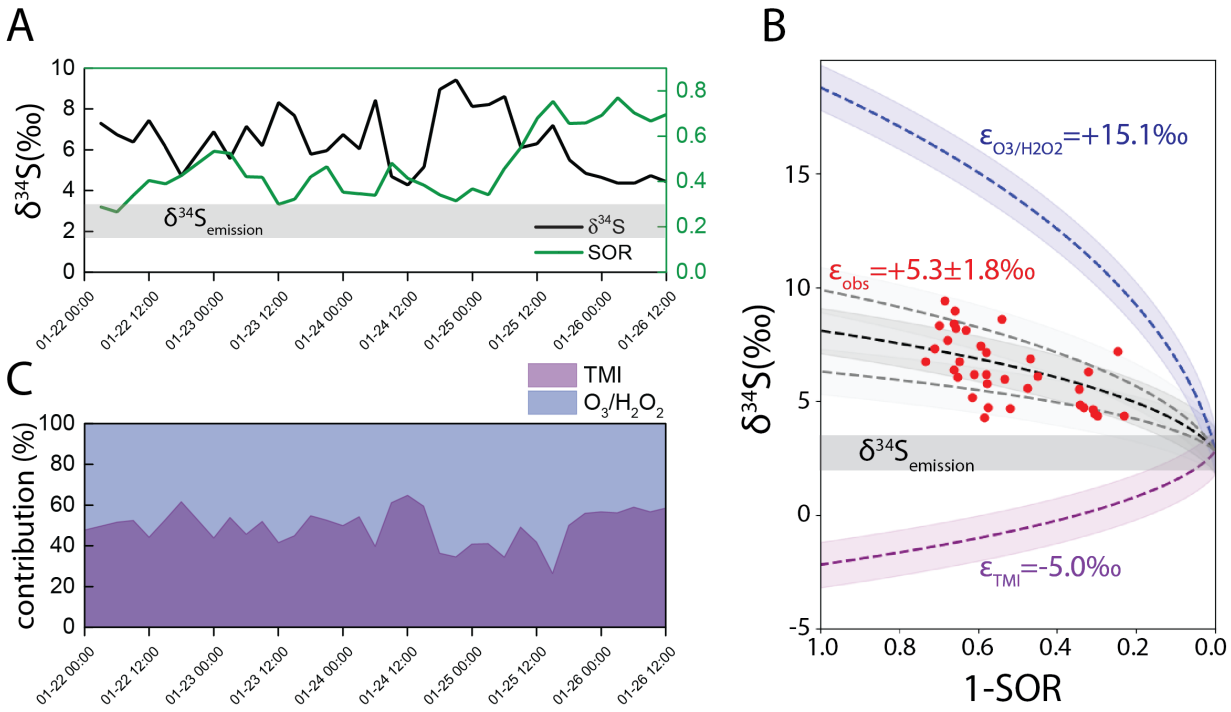

Fig 3. A) measured $\delta^{34}S_{sulfate}$ (black), calculated sulfur oxidation ratio (SOR, green) throughout the sampling period; and compare with estimated $\delta^{34}S_{emission}$ (grey bar); B) Rayleigh distillation model of sulfate production. Grey bar indicates the $\delta^{34}S_{emission}$ (+2.7±1.0‰) in Nanjing, red circles are the measured $\delta^{34}S_{sulfate}$ in this study. Dashed lines with shaded areas are calculated $\delta^{34}S_{sulfate}$ values based on the $\delta^{34}S_{emission}$: blue line indicates the $\delta^{34}S_{sulfate}$ when SO_2 is oxidized solely by O_3 and H_2O_2, purple line indicates the $\delta^{34}S_{sulfate}$ when SO_2 is oxidized solely by TMI oxidation, black line is the estimated ε value of +5.3‰ and two grey lines represent the upper and lower limit for the estimated ε values (+3.5‰ and +7.1‰).

References:

(1) Zheng, B.; Zhang, Q.; Zhang, Y.; He, K. B.; Wang, K.; Zheng, G. J.; Duan, F. K.; Ma, Y. L.; Kimoto, T. Heterogeneous Chemistry: A Mechanism Missing in Current Models to Explain Secondary Inorganic Aerosol Formation during the January 2013 Haze Episode in North China. *Atmos. Chem. Phys.* **2015**, *15* (4), 2031-2049.

(2) Guo, S.; Hu, M.; Zamora, M. L.; Peng, J.; Shang, D.; Zheng, J.; Du, Z.; Wu, Z.; Shao, M.; Zeng, L. Elucidating Severe Urban Haze Formation in China. *Proc. Natl. Acad. Sci.* **2014**, *111* (49), 17373–17378.

(3) Zheng, G. J.; Duan, F. K.; Su, H.; Ma, Y. L.; Cheng, Y.; Zheng, B.; Zhang, Q.; Huang, T.; Kimoto, T.; Chang, D. Exploring the Severe Winter Haze in Beijing: The Impact of Synoptic Weather, Regional Transport and Heterogeneous Reactions. *Atmos. Chem. Phys.* **2015**, *15* (6), 2969–2983.

(4) Huang, R.-J.; Zhang, Y.; Bozzetti, C.; Ho, K.-F.; Cao, J.-J.; Han, Y.; Daellenbach, K. R.; Slowik, J. G.; Platt, S. M.; Canonaco, F. High Secondary Aerosol Contribution to Particulate Pollution during Haze Events in China. *Nature* **2014**, *514* (7521), 218.

(5) Atkinson, R.; Baulch, D. L.; Cox, R. A.; Crowley, J. N.; Hampson, R. F.; Hynes, R. G.; Jenkin, M. E.; Rossi, M. J.; Troe, J. Evaluated Kinetic and Photochemical Data for Atmospheric Chemistry: Volume I-Gas Phase Reactions of Ox, HOx, NOx and SOx Species. *Atmos. Chem. Phys.* **2004**, *4* (6), 1461–1738.

(6) Reid, J. S.; Jonsson, H. H.; Smith, M. H.; Smirnov, A. Evolution of the Vertical Profile and Flux of Large Sea-salt Particles in a Coastal Zone. *J. Geophys. Res. Atmos.* **2001**, *106* (D11), 12039–12053.

(7) Herrmann, H.; Ervens, B.; Jacobi, H.-W.; Wolke, R.; Nowacki, P.; Zellner, R. CAPRAM2. 3: A Chemical Aqueous Phase Radical Mechanism for Tropospheric Chemistry. *J. Atmos. Chem.* **2000**, *36* (3), 231–284.

(8) Sofen, E. D.; Alexander, B.; Kunasek, S. A. The Impact of Anthropogenic Emissions on Atmospheric Sulfate Production Pathways, Oxidants, and Ice Core $\Delta^{17}O$ (SO_4^{2-}). *Atmos. Chem. Phys.* **2011**, *11* (7), 3565–3578.

(9) Harris, E.; Sinha, B.; Pinxteren, D. Van; Tilgner, A.; Fomba, K. W.; Schneider, J.; Roth, A.; Gnauk, T.; Fahlbusch, B.; Mertes, S., Lee, T., Collett, J., Foley, S., Borrmann, S., Hoppe, P., Herrmann, H.; Enhanced Role of Transition Metal Ion Catalysis during In-Cloud Oxidation of SO_2. *Science (80-.).* **2013**, *340* (6133), 727–730. https://doi.org/10.1126/science.1230911.

(10) Alexander, B.; Park, R. J.; Jacob, D. J.; Gong, S. Transition Metal-Catalyzed Oxidation of Atmospheric Sulfur: Global Implications for the Sulfur Budget. *J. Geophys. Res.* **2009**, *114* (D2), D02309. https://doi.org/10.1029/2008JD010486.

(11) Wang, G., Zhang, R., Gomez, M., Yang, L., Levy Zamora, M., Hu, M., Lin, Y., Peng, J., Guo, S., Meng, J., Li, J., Cheng, C., Hu, T., Ren, Y., Wang, Y., Gao, J., Cao, J., An, Z., Zhou, W., Li, G., Wang, J., Tian, P., Marrero-Ortiz, W., Secrest, J., Du, Z., Zheng, J., Shang, D., Zeng, L., Shao, M., Wang, W., Huang, Y., Wang, Y., Zhu, Y., Li, Y., Hu, J., Pan, B., Cai, L., Cheng, Y., Ji, Y., Zhang, F., Rosenfeld, D., Liss, P., Duce, R., Kolb, C., Molina, M., Persistent Sulfate Formation from London Fog to Chinese Haze. *Proc. Natl. Acad. Sci. U. S. A.* **2016**, 201616540. https://doi.org/10.1073/pnas.1616540113.

(12) Cheng, Y.; Zheng, G.; Wei, C.; Mu, Q.; Zheng, B.; Wang, Z.; Gao, M.; Zhang, Q.; He, K.;

Carmichael, G. Reactive Nitrogen Chemistry in Aerosol Water as a Source of Sulfate during Haze Events in China. *Sci. Adv.* **2016**, *2* (12), e1601530.

(13) Xue, J.; Yuan, Z.; Yu, J. Z.; Lau, A. K. H. An Observation-Based Model for Secondary Inorganic Aerosols. *Aerosol Air Qual. Res.* **2014**, *14*, 862–878. https://doi.org/10.4209/aaqr.2013.06.0188.

(14) Xue, J.; Yuan, Z.; Griffith, S. M.; Yu, X.; Lau, A. K. H.; Yu, J. Z. Sulfate Formation Enhanced by a Cocktail of High NO_x, SO_2 , Particulate Matter, and Droplet PH during Haze-Fog Events in Megacities in China: An Observation-Based Modeling Investigation. *Environ. Sci. Technol.* **2016**, *50* (14), 7325–7334. https://doi.org/10.1021/acs.est.6b00768.

(15) Li, G.; Bei, N.; Cao, J.; Huang, R.; Wu, J.; Feng, T.; Wang, Y.; Liu, S.; Zhang, Q.; Tie, X. A Possible Pathway for Rapid Growth of Sulfate during Haze Days in China. *Atmos. Chem. Phys.* **2017**, *17* (5), 3301–3316.

(16) Huang, X.; Song, Y.; Zhao, C.; Li, M.; Zhu, T.; Zhang, Q.; Zhang, X. Pathways of Sulfate Enhancement by Natural and Anthropogenic Mineral Aerosols in China. *J. Geophys. Res. Atmos.* **2014**, *119* (24), 14,165-14,179. https://doi.org/10.1002/2014JD022301.

(17) He, P.; Alexander, B.; Geng, L.; Chi, X.; Fan, S.; Zhan, H.; Kang, H.; Zheng, G.; Cheng, Y.; Su, H., Liu, C., Xie, Z. Isotopic Constraints on Heterogeneous Sulfate Production in Beijing Haze. *Atmos. Chem. Phys.* **2018**, *18* (8), 5515–5528. https://doi.org/10.5194/acp-18-5515-2018.

(18) Li, L.; Hoffmann, M. R.; Colussi, A. J. Role of Nitrogen Dioxide in the Production of Sulfate during Chinese Haze-Aerosol Episodes. https://doi.org/10.1021/acs.est.7b05222.

(19) Liu, C.; Ma, Q.; Liu, Y.; Ma, J.; He, H. Synergistic Reaction between SO_2 and NO_2 on Mineral Oxides: A Potential Formation Pathway of Sulfate Aerosol. *Phys. Chem. Chem. Phys.* **2012**, *14* (5), 1668–1676.

(20) Zhao, D.; Song, X.; Zhu, T.; Zhang, Z.; Liu, Y.; Shang, J. Multiphase Oxidation of SO_2 by NO_2 on $CaCO_3$ Particles. *Atmos. Chem. Phys.* **2018**, *18* (4), 2481–2493.

(21) Wang, G.; Huang, L.; Gao, S.; Gao, S.; Wang, L. Characterization of Water-Soluble Species of PM_{10} and $PM_{2.5}$ Aerosols in Urban Area in Nanjing, China. *Atmos. Environ.* **2002**, *36* (8), 1299–1307.

(22) Shao, J.; Chen, Q.; Wang, Y.; Lu, X.; He, P.; Sun, Y.; Shah, V.; Martin, R. V; Philip, S.; Song, S. Heterogeneous Sulfate Aerosol Formation Mechanisms during Wintertime Chinese Haze Events: Air Quality Model Assessment Using Observations of Sulfate Oxygen Isotopes in Beijing. *Atmos. Chem. Phys.* **2019**, *19* (9), 6107–6123.

(23) Li, X.; Bao, H.; Gan, Y.; Zhou, A.; Liu, Y. Multiple Oxygen and Sulfur Isotope Compositions of Secondary Atmospheric Sulfate in a Mega-City in Central China. *Atmos. Environ.* **2013**, *81*, 591–599.

(24) Zhang, R.; Wang, G.; Guo, S.; Zamora, M. L.; Ying, Q.; Lin, Y.; Wang, W.; Hu, M.; Wang, Y. Formation of Urban Fine Particulate Matter. *Chem. Rev.* **2015**, *115* (10), 3803–3855.

(25) Wang, J.; Wang, S.; Jiang, J.; Ding, A.; Zheng, M.; Zhao, B.; Wong, D. C.; Zhou, W.; Zheng, G.; Wang, L. Impact of Aerosol–Meteorology Interactions on Fine Particle Pollution during China's Severe Haze Episode in January 2013. *Environ. Res. Lett.* **2014**, *9* (9), 94002.

(26) Wang, Y.; Zhang, Q.; Jiang, J.; Zhou, W.; Wang, B.; He, K.; Duan, F.; Zhang, Q.; Philip, S.; Xie, Y. Enhanced Sulfate Formation during China's Severe Winter Haze Episode in January 2013 Missing from Current Models. *J. Geophys. Res. Atmos.* **2014**, *119* (17), 10–

425.
(27) Liu, M.; Song, Y.; Zhou, T.; Xu, Z.; Yan, C.; Zheng, M.; Wu, Z.; Hu, M.; Wu, Y.; Zhu, T. Fine Particle PH during Severe Haze Episodes in Northern China. *Geophys. Res. Lett.* **2017**, *44* (10), 5213–5221.
(28) Shi, G.; Xu, J.; Peng, X.; Xiao, Z.; Chen, K.; Tian, Y.; Guan, X.; Feng, Y.; Yu, H.; Nenes, A. PH of Aerosols in a Polluted Atmosphere: Source Contributions to Highly Acidic Aerosol. *Environ. Sci. Technol.* **2017**, *51* (8), 4289–4296.
(29) Weber, R. J.; Guo, H.; Russell, A. G.; Nenes, A. High Aerosol Acidity despite Declining Atmospheric Sulfate Concentrations over the Past 15 Years. *Nat. Geosci.* **2016**, *9* (4), 282.
(30) Fountoukis, C.; Nenes, A. ISORROPIA II: A Computationally Efficient Thermodynamic Equilibrium Model for K^+–Ca^{2+}–Mg^{2+}–NH_4^+–Na^+–SO_4^{2-}–NO_3^-–Cl^-–H_2O Aerosols. *Atmos. Chem. Phys.* **2007**, *7* (17), 4639–4659.
(31) Seinfeld, J. H.; Pandis, S. N.; Noone, K. Atmospheric Chemistry and Physics: From Air Pollution to Climate Change. AIP 1998, pp 265-324.
(32) Gankanda, A.; Coddens, E. M.; Zhang, Y.; Cwiertny, D. M.; Grassian, V. H. Sulfate Formation Catalyzed by Coal Fly Ash, Mineral Dust and Iron (Iii) Oxide: Variable Influence of Temperature and Light. *Environ. Sci. Process. Impacts* **2016**, *18* (12), 1484–1491.
(33) Bao, H.; Thiemens, M. H.; Loope, D. B.; Yuan, X.-L. Sulfate Oxygen-17 Anomaly in an Oligocene Ash Bed in Mid-North America: Was It the Dry Fogs? *Geophys. Res. Lett.* **2003**, *30* (16). https://doi.org/10.1029/2003GL016869.
(34) Bao, H.; Reheis, M. C. Multiple Oxygen and Sulfur Isotopic Analyses on Water-Soluble Sulfate in Bulk Atmospheric Deposition from the Southwestern United States. *J. Geophys. Res. D Atmos.* **2003**, *108* (14), 4430. https://doi.org/10.1029/2002jd003022.
(35) Harris, E.; Sinha, B.; Hoppe, P.; Ono, S. High-Precision Measurements of ^{33}S and ^{34}S Fractionation during SO_2 Oxidation Reveal Causes of Seasonality in SO_2 and Sulfate Isotopic Composition. *Environ. Sci. Technol.* **2013**, *47* (21), 12174–12183. https://doi.org/10.1021/es402824c.
(36) Harris, E.; Sinha, B.; Hoppe, P.; Foley, S.; Borrmann, S. Fractionation of Sulfur Isotopes during Heterogeneous Oxidation of SO_2 on Sea Salt Aerosol: A New Tool to Investigate Non-Sea Salt Sulfate Production in the Marine Boundary Layer. *Atmos. Chem. Phys. Atmos. Chem. Phys.* **2012**, *12*, 4619–4631. https://doi.org/10.5194/acp-12-4619-2012.
(37) Harris, E.; Sinha, B.; Hoppe, P.; Crowley, J. N.; Ono, S.; Foley, S. Sulfur Isotope Fractionation during Oxidation of Sulfur Dioxide: Gas-Phase Oxidation by OH Radicals and Aqueous Oxidation by H_2O_2, O_3 and Iron Catalysis. *Atmos. Chem. Phys. Atmos. Chem. Phys.* **2012**, *12*, 407–424. https://doi.org/10.5194/acp-12-407-2012.
(38) Guo, Z.; Shi, L.; Chen, S.; Jiang, W.; Wei, Y.; Rui, M.; Zeng, G. Sulfur Isotopic Fractionation and Source Appointment of $PM_{2.5}$ in Nanjing Region around the Second Session of the Youth Olympic Games. *Atmos. Res.* **2016**, *174*, 9–17.
(39) Chen, S.; Guo, Z.; Guo, Z.; Guo, Q.; Zhang, Y.; Zhu, B.; Zhang, H. Sulfur Isotopic Fractionation and Its Implication: Sulfate Formation in $PM_{2.5}$ and Coal Combustion under Different Conditions. *Atmos. Res.* **2017**, *194*, 142–149.
(40) Li, J.; Michalski, G.; Davy, P.; Harvey, M.; Katzman, T.; Wilkins, B. Investigating Source Contributions of Size-Aggregated Aerosols Collected in Southern Ocean and Baring Head, New Zealand Using Sulfur Isotopes. *Geophys. Res. Lett.* **2018**, *45*(8), 3717-3727.
(41) Saltzman, E. S.; Brass, G. W.; Price, D. A. The Mechanism of Sulfate Aerosol Formation:

Chemical and Sulfur Isotopic Evidence. *Geophys. Res. Lett.* **1983**, *10* (7), 513–516. https://doi.org/10.1029/GL010i007p00513.

(42) Rayleigh, Lord. L. Theoretical Considerations Respecting the Separation of Gases by Diffusion and Similar Processes. *London, Edinburgh, Dublin Philos. Mag. J. Sci.* **1896**, *42* (259), 493–498.

(43) Maruyama, T.; Ohizumi, T.; Taneoka, Y.; Minami, N.; Fukuzaki, N.; Mukai, H.; Murano, K.; Kusakabe, M. Sulfur Isotope Ratios of Coals and Oils Used in China and Japan. *Nippon Kagaku Kaishi* **2000**, No. 1, 45–52.

(44) Mukai, H.; Tanaka, A.; Fujii, T.; Zeng, Y.; Hong, Y.; Tang, J.; Guo, S.; Xue, H.; Sun, Z.; Zhou, J. Regional Characteristics of Sulfur and Lead Isotope Ratios in the Atmosphere at Several Chinese Urban Sites. *Environ. Sci. Technol.* **2001**, *35* (6), 1064–1071.

(45) Han, X.; Guo, Q.; Liu, C.; Fu, P.; Strauss, H.; Yang, J.; Hu, J.; Wei, L.; Ren, H.; Peters, M. Using Stable Isotopes to Trace Sources and Formation Processes of Sulfate Aerosols from Beijing, China. *Sci. Rep.* **2016**, *6*, 29958.

(46) Wei, L.; Yue, S.; Zhao, W.; Yang, W.; Zhang, Y.; Ren, L.; Han, X.; Guo, Q.; Sun, Y.; Wang, Z.; Fu, P.; Stable Sulfur Isotope Ratios and Chemical Compositions of Fine Aerosols ($PM_{2.5}$) in Beijing, China. *Science of The Total Environment*, **2018,** 633, 1156-1164. https://doi.org/10.1016/j.scitotenv.2018.03.153.

(47) Guo, Z.; Li, Z.; Farquhar, J.; Kaufman, A. J.; Wu, N.; Li, C.; Dickerson, R. R.; Wang, P. Identification of Sources and Formation Processes of Atmospheric Sulfate by Sulfur Isotope and Scanning Electron Microscope Measurements. *J. Geophys. Res.* **2010**, *115* (D7), D00K07. https://doi.org/10.1029/2009JD012893.

(48) Han, X.; Guo, Q.; Strauss, H.; Liu, C.; Hu, J.; Guo, Z.; Wei, R.; Peters, M.; Tian, L.; Kong, J. Multiple Sulfur Isotope Constraints on Sources and Formation Processes of Sulfate in Beijing PM2. 5 Aerosol. *Environ. Sci. Technol.* **2017**, *51* (14), 7794–7803.

(49) Lin, M.; Biglari, S.; Zhang, Z.; Crocker, D.; Tao, J.; Su, B.; Liu, L.; Thiemens, M. H. Vertically Uniform Formation Pathways of Tropospheric Sulfate Aerosols in East China Detected from Triple Stable Oxygen and Radiogenic Sulfur Isotopes. *Geophys. Res. Lett.* **2017**, *44* (10), 5187–5196. https://doi.org/10.1002/2017GL073637.

(50) Lin, M.; Zhang, X.; Li, M.; Xu, Y.; Zhang, Z.; Tao, J.; Su, B.; Liu, L.; Shen, Y.; Thiemens, M. H. Five-S-Isotope Evidence of Two Distinct Mass-Independent Sulfur Isotope Effects and Implications for the Modern and Archean Atmospheres. *Proc. Natl. Acad. Sci.* **2018**, *115* (34), 8541–8546.

(51) Romero, A. B.; Thiemens, M. H. Mass-independent Sulfur Isotopic Compositions in Present-day Sulfate Aerosols. *J. Geophys. Res. Atmos.* **2003**, *108* (D16), 4524.

(52) Cao, F.; Zhang, S.-C.; Kawamura, K.; Zhang, Y.-L. Inorganic Markers, Carbonaceous Components and Stable Carbon Isotope from Biomass Burning Aerosols in Northeast China. *Sci. Total Environ.* **2016**, *572*, 1244–1251.

(53) Legrand, M.; Hammer, C.; De Angelis, M.; Savarino, J.; Delmas, R.; Clausen, H.; Johnsen, S. J. Sulfur-containing Species (Methanesulfonate and SO_4) over the Last Climatic Cycle in the Greenland Ice Core Project (Central Greenland) Ice Core. *J. Geophys. Res. Ocean.* **1997**, *102* (C12), 26663–26679.

(54) Calhoun, J. A.; Bates, T. S.; Charlson, R. J. Sulfur Isotope Measurements of Submicrometer Sulfate Aerosol Particles over the Pacific Ocean. *Geophys. Res. Lett.* **1991**, *18* (10), 1877–1880. https://doi.org/10.1029/91GL02304.

(55) Faloona, I. Sulfur Processing in the Marine Atmospheric Boundary Layer: A Review and

Critical Assessment of Modeling Uncertainties. *Atmos. Environ.* **2009**, *43* (18), 2841–2854. https://doi.org/10.1016/j.atmosenv.2009.02.043.

(56) Li, M.; Zhang, Q.; Kurokawa, J.; Woo, J.-H.; He, K.; Lu, Z.; Ohara, T.; Song, Y.; Streets, D. G.; Carmichael, G. R. MIX: A Mosaic Asian Anthropogenic Emission Inventory under the International Collaboration Framework of the MICS-Asia and HTAP. *Atmos. Chem. Phys.* **2017**, *17* (2), 935-963.

(57) Hong, Y.; Zhang, H.; Zhu, Y. Sulfur Isotopic Characteristics of Coal in China and Sulfur Isotopic Fractionation during Coal-Burning Process. *Chinese J. geochemistry* **1993**, *12* (1), 51–59.

(58) Novák, M.; Jacková, I.; Prechová, E. Temporal Trends in the Isotope Signature of Air-Borne Sulfur in Central Europe. *Environ. Sci. Technol.* **2001**, *35* (2), 255–260.

(59) Forrest, J.; Newman, L. Sampling and Analysis of Atmospheric Sulfur Compounds for Isotope Ratio Studies. *Atmos. Environ.* **1973**, *7* (5), 561–573.

(60) Mariotti, A.; Germon, J. C.; Hubert, P.; Kaiser, P.; Letolle, R.; Tardieux, A.; Tardieux, P. Experimental Determination of Nitrogen Kinetic Isotope Fractionation: Some Principles; Illustration for the Denitrification and Nitrification Processes. *Plant Soil* **1981**, *62* (3), 413–430.

(61) Madronich, S.; Flocke, S. The Role of Solar Radiation in Atmospheric Chemistry. In *Environmental photochemistry*; Springer, 1999; pp 1–26.

(62) Stockwell, W. R.; Kirchner, F.; Kuhn, M.; Seefeld, S. A New Mechanism for Regional Atmospheric Chemistry Modeling. *J. Geophys. Res. Atmos.* **1997**, *102* (D22), 25847–25879.

(63) Heard, D. E.; Carpenter, L. J.; Creasey, D. J.; Hopkins, J. R.; Lee, J. D.; Lewis, A. C.; Pilling, M. J.; Seakins, P. W.; Carslaw, N.; Emmerson, K. M. High Levels of the Hydroxyl Radical in the Winter Urban Troposphere. *Geophys. Res. Lett.* **2004**, *31* (18), L18112.

(64) Ren, X.; Brune, W. H.; Mao, J.; Mitchell, M. J.; Lesher, R. L.; Simpas, J. B.; Metcalf, A. R.; Schwab, J. J.; Cai, C.; Li, Y. Behavior of OH and HO_2 in the Winter Atmosphere in New York City. *Atmos. Environ.* **2006**, *40*, 252–263.

(65) Giardina, M.; Buffa, P. A New Approach for Modeling Dry Deposition Velocity of Particles. *Atmos. Environ.* **2018**, *180*, 11–22.

(66) Han, S.; Wu, J.; Zhang, Y.; Cai, Z.; Feng, Y.; Yao, Q.; Li, X.; Liu, Y.; Zhang, M. Characteristics and Formation Mechanism of a Winter Haze–Fog Episode in Tianjin, China. *Atmos. Environ.* **2014**, *98*, 323–330.

(67) Zhang, C.; Wang, L.; Qi, M.; Ma, X.; Zhao, L.; Ji, S.; Wang, Y.; Lu, X.; Wang, Q.; Xu, R. Evolution of Key Chemical Components in $PM_{2.5}$ and Potential Formation Mechanisms of Serious Haze Events in Handan, China. *Aerosol Air Qual. Res.* **2018**, *18*, 1545–1557.

(68) Jacob, D. J. Heterogeneous Chemistry and Tropospheric Ozone. *Atmos. Environ.* **2000**, *34* (12–14), 2131–2159.

(69) Fu, H.; Wang, X.; Wu, H.; Yin, Y.; Chen, J. Heterogeneous Uptake and Oxidation of SO2 on Iron Oxides. *J. Phys. Chem. C* **2007**, *111* (16), 6077–6085.

(70) Adams, J. W.; Rodriguez, D.; Cox, R. A. The Uptake of SO 2 on Saharan Dust: A Flow Tube Study. *Atmos. Chem. Phys.* **2005**, *5* (10), 2679–2689.

(71) Shanquan, L. I.; ZHANG, G.; Jinling, Y.; Nan, J. I. A. Multi-Source Characteristics of Atmospheric Deposition in Nanjing, China, as Controlled by East Asia Monsoons and Urban Activities. *Pedosphere* **2016**, *26* (3), 374–385.

(72) Amiri, N.; Ghahremaninezhad, R.; Rempillo, O.; Tokarek, T. W.; Odame-Ankrah, C. A.; Osthoff, H. D.; Norman, A.-L. Stable Sulfur Isotope Measurements to Trace the Fate of SO 2 in the Athabasca Oil Sands Region. *Atmos. Chem. Phys.* **2018**, *18* (11), 7757–7780.